Crystallization Behavior and Its Influence on the Mechanical Properties of a Thermoplastic Elastomer Produced by *Pseudomonas oleovorans*

K. D. Gagnon,* R. W. Lenz, and R. J. Farris

Polymer Science and Engineering Department, University of Massachusetts, Amherst, Massachusetts 01003

R. C. Fuller

Biochemistry and Molecular Biology Department, University of Massachusetts, Amherst, Massachusetts 01003

Received December 26, 1991; Revised Manuscript Received April 6, 1992

ABSTRACT: An investigation was conducted into the crystallization kinetics of PHO, poly(β-hydroxyoctanoate), a bacterially produced copolyester containing mostly β-hydroxyoctanoate repeating units. The crystallization rate reached a maximum at 0–5 °C. The equilibrium melting point was determined to be approximately 68 °C. The long-term crystallization study on PHO crystallized from the melt at −20, +5, and +20 °C revealed that stable but different levels of crystallinity were reached after 3–7 weeks. The melting endotherm peak continued to change shape for up to 19 weeks. After 24 weeks of crystallization, the mechanical properties of the films were evaluated. The tensile modulus ranged from 2.5 to 9 MPa, the tensile strength at break from 6 to 10 MPa, and the ultimate elongation from 450% to 300%. A high tensile set, approximately 35% after 100% elongation, was observed for PHO crystallized at all three temperatures. Unusual melting endotherm peak shapes were observed for long-term crystallized samples after undergoing large extensions.

Introduction

Polyesters produced by bacteria are poly(β-hydroxyalkanoates) or PHAs. *Pseudomonas oleovorans*, when grown on sodium octanoate[1,2] or octane[3–7] as the sole carbon source, produces a copolymer containing mostly β-hydroxyoctanoate repeating units, PHO. The polymer is accumulated as intracellular granules in response to an environmental stress such as nutrient limitations or a lack of oxygen.[4,8]

Because PHO is naturally produced and degraded by bacteria in response to environmental changes, the polymer is inherently biodegradable. Biodegradability of the polymer after extraction from the native bacteria and formation into a desired product is expected in a manner similar to that of the commercially available poly(β-hydroxybutyrate), PHB, and poly(β-hydroxybutyrate-*co*-β-hydroxyvalerate), PHB/HV, which are bacterially produced thermoplastic polymers.[9–11] The copolymer produced when the bacteria are grown on sodium octanoate has a random[12] repeat unit structure and the composition shown in Figure 1.[1] *P. oleovorans* has the ability to incorporate the long alkyl chain of the carbon source into the repeat unit structure as a pendant group always in the absolute [R] configuration and located at the β position to the carbonyl carbon.[4] Because these repeating units are all in the same stereochemical configuration, the polymer is isotactic, making crystallization possible. However, the overall crystallizability of the polymer is reduced because PHO is a copolymer and not a homopolymer.

Thermal history greatly affects the mechanical properties of semicrystalline polymers mainly due to the changes in crystallinity. Thermal conditions can affect the crystalline growth rate, resulting crystallite size, and final degree of crystallinity. Annealing polymers to increase lamellar thickness, increase the purity or perfection of the crystalline regions, and increase the overall degree of crystallinity is well-known.[14–16] PHO has a glass transition temperature at −35 °C,[1] a melting temperature at 61 °C,[2] and approximately a 30% degree of crystallinity.[13] Rubbery behavior is observed at room temperature where the crystalline regions act as physical cross-links, and therefore PHO has been described as a thermoplastic elastomer.

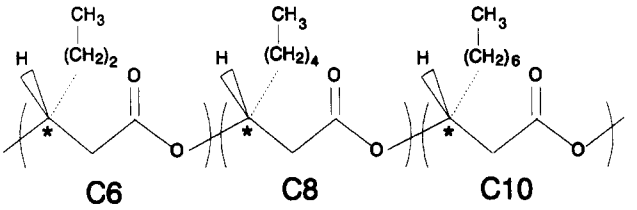

Composition	Description of Repeat Units
10%	C6 = beta-hydroxyhexanoate
86%	C8 = beta-hydroxyoctanoate
4%	C10 = beta-hydroxydecanoate

Figure 1. Stereochemical representation of the structure of PHO with the percent composition of repeat units indicated. C(#) indicates the number of carbon atoms present in the repeat unit.

Because the crystalline regions of PHO act as physical cross-links, an investigation into crystallization behavior as a function of temperature was conducted. The rate of crystallization was investigated over a range of temperatures to determine the temperature at which the crystallization rate is at a maximum and to estimate the theoretical maximum melting temperature (equilibrium melting temperature). A long-term crystallization study was conducted on PHO films to determine the time required to reach a maximum level of crystallinity, to

0024-9297/92/2225-3723$03.00/0

measure the levels of crystallinity obtainable at the different crystallization temperatures, and to measure the effect of different thermal histories on the mechanical properties of this material. Tensile set, an indication of the inelastic nature of the material, was also evaluated. A thermal analysis of these stretched samples was conducted to observe any changes to the crystalline regions after extension.

Experimental Section

Materials. PHO was produced by *P. oleovorans* using sodium octanoate in a fed batch type fermentation biosynthesis.[17] The lyophilized biomass was extracted in chloroform and purified by precipitating in methanol.

Three films of PHO, 1–1.5 mm thick, were prepared by solution casting from a 15–30% chloroform solution. The solutions were filtered through a 10-μm filter into a glass casting dish. Filtering was conducted in an attempt to remove possible contaminants which could act as nucleating agents. One additional film of PHO, 1 mm thick, was solution cast with 0.5% talc to act as a nucleating agent. The solution was filtered through a 5-μm filter in an attempt to limit the size of the talc particles. The type, amount, and size of the nucleating agent were chosen as suggested by its use with other polyesters.[18] For all cast films, the solvent was allowed to slowly evaporate at room temperature over the course of 7–10 days.

Methods and Procedures. DSC Analysis. Differential scanning calorimetry was conducted using a TA Instruments DSC Model 2910. Mercury was used as the low-temperature calibation standard. Unless noted otherwise, the test method involved heating 10–15-mg samples at 20 °C/min from −85 to +90 °C.

Crystallization Rate Study. For the crystallization rate study, the DSC samples sealed in hermetic pans were melted at 80 °C for 3–5 min in the DSC cell. The samples were then sealed in glass vials. The vials were attached to a steel plate via copper wire and submersed in the appropriate temperature bath. Three to six samples were tested at each temperature. The temperature baths used depended on the temperature desired: for −40 to +20 °C, a Cryocool coil was submersed in an ethanol bath; for 25–40 °C, a water bath heated using a temperature-controlled hot plate was used. After 24 h, the samples were removed from the temperature baths, one by one, and analyzed using the DSC.

Long-Term Crystallization Study. DSC samples were taken from each of the four solution-cast films and sealed in hermetic pans. The pans were then sealed in glass vials. The solution-cast films, which remained in the glass casting dishes fitted with glass covers, and the DSC samples in the glass vials were melted overnight at 75 °C in a vacuum oven. The films in the covered glass casting dishes were double bagged in ziplock bags. The films and DSC samples were placed in or submersed into the appropriate temperature baths to crystallize. The temperature baths used were as follows: for −20 °C, freezer portion of a refrigerator; for 5 °C, refrigerator portion of a refrigerator; for 20 °C, a Cryocool coil submersed in methanol/water bath. The DSC samples were evaluated periodically to monitor the level of crystallinity by measurement of the heat of fusion, ΔH_m.

Tensile Testing. After 24 weeks the films were removed from the temperatures baths and allowed to equilibrate at room temperature. All tensile testing was conducted using an Instron Universal Testing Instrument Model TTBM with an Interface SM-50 load cell. Ring samples per ASTM D 412, Type 2, were punched from the films using a steel rule die and Carver Hot Press Model C at room temperature.[19] Special grips were made to hold the ring specimens. The ring was supported at each end by a pin, approximately 5 mm in diameter. Each pin was engaged at both ends in the inner track of a ball bearing to ensure the stress and strain remained equal on both sides of the ring during testing. The pins are removable for loading the sample. The initial gauge length was based on half the average circumference of the ring die. A strain rate of 1 min^{-1} was used for all tensile tests.

Tensile Set Testing. After 28 weeks of crystallization, strip samples, 50 mm wide, were cut from the films and evaluated for tensile set. All tensile set testing was conducted using an Instron Universal Testing Instrument Model TTBM with an Interface SM-50 load cell. Tensile set testing procedures were based on the procedures described in ASTM D412.[19] Different crosshead speeds were used to reach the desired elongation within approximately 15 s. Grip slippage was a problem for the elastomers, and since no extensiometer was available, a ruler was held next to the sample to ensure the marked gauge length reached the desired elongation. The samples were held for 10 min at the intended elongation and then released at the same crosshead speed. The samples were then allowed to recover for 10 min prior to final measurement of the gauge length. Tensile set was determined as the percent change in the marked gauge length of the samples. Tensile set at break was also determined from the ring samples which had undergone tensile testing and was calculated as the percent change in the mean circumference of the samples.

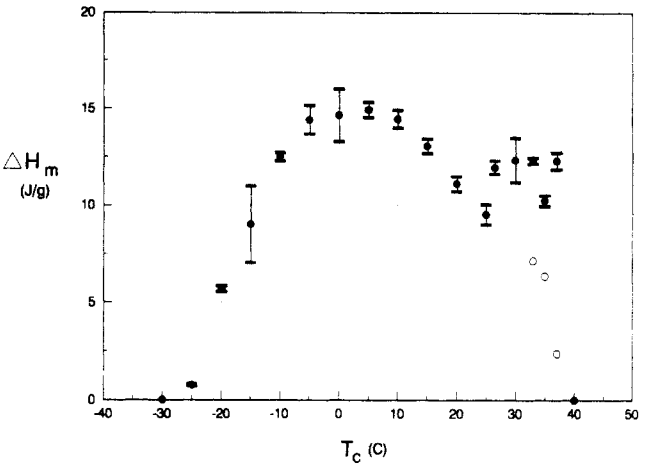

Figure 2. Variation in the heat of fusion, ΔH_m, with the crystallization temperature, T_c, for PHO crystallized for 24 h from the melt. Solid symbols represent the average values from three to six samples. Open symbols represent single data points. Error bars indicate ±1 standard deviation.

Results and Discussion

Crystallization Rate. Unlike PHB,[20] PHO does not exhibit spherulitic texture[13] and the literature to date has only described the crystallization rate qualitatively as requiring 3 days[13] to weeks[2] to fully crystallize at room temperature.

In order to determine crystallization rates, all samples were melted and then allowed to crystallize at different temperatures. After 24 h, a DSC thermogram was obtained to determine the heat of fusion (a proportional indication of the level of crystallinity) which had developed in the 24-h period. Because all samples were compared after 24 h and because crystallization was not complete in that period of time, relative rates of crystallization could be determined.

The results of the experiment are depicted in Figures 2–4. Figure 2 shows the variation in the heat of fusion, ΔH_m, with the crystallization temperature, T_c. As expected, a bell-shaped curve resulted, with the rate reaching a maximum at approximately the median between the glass transition temperature at −35 °C and the melting temperature at 61 °C. The location of the peak indicates that the fastest crystallization rate occurred at 0–5 °C.

At temperatures above 25 °C, scatter in the data was noted. The three open circles indicate data points from single samples. The solid circles indicate an average of the values from three to six samples. The extent of crystallinity in the majority of samples crystallized from 25 to 37 °C was higher than expected. Impurities can act as nucleating agents, and, even though filtering of the

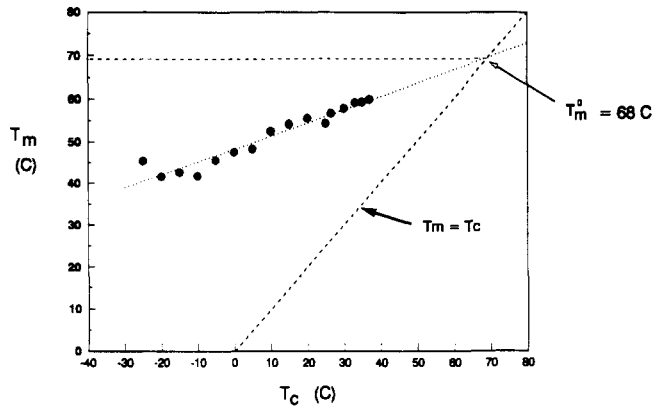

Figure 3. Melting temperature, T_m, as a function of the crystallization temperature, T_c, for PHO crystallized for 24 h from the melt.

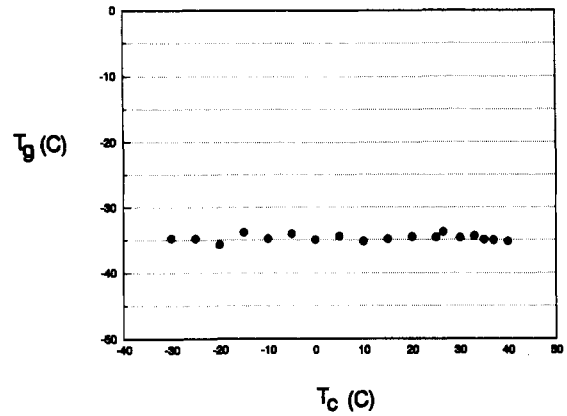

Figure 4. Glass transition temperature, T_g, as a function of the crystallization temperature, T_c, for PHO crystallized for 24 h from the melt.

polymer solutions prior to film casting was conducted, all impurities may not have been removed. These undesired nucleating agents would have a more profound effect at the higher temperatures where nucleation can limit the rate of crystallization. These nuclei would enable a higher than expected extent of crystallization to occur during the 24 h, thereby contributing to the data scatter. Annealing effects are not significant, neither during the DSC scan nor during the initial 24 h of crystallization, as will be shown in the long-term crystallization study results. Crystallization at lower temperatures is generally limited by chain mobility and not by nucleation, so impurities acting as nucleation sites would not have as much effect on the extent of crystallization in 24 h. In this case data scatter would not be expected and, in fact, was not observed.

Figure 3 depicts the change in the melting temperature, T_m, as a function of the crystallization temperature, T_c. The melting temperature varied with the crystallization temperature in a manner common for all polymers.[15] The line shown through the data was determined by linear regression, and the intersection of this line with the theoretical $T_m = T_c$ line was used to estimate the equilibrium melting point. The equilibrium melting point of PHO was determined to be approximately 68 °C using this construction. Figure 4 shows that, as expected, the glass transition temperature, T_g, did not vary significantly with the crystallization temperature, T_c.

Long-Term Crystallization Study. PHO films crystallized at three different temperatures were evaluated for crystallization development and mechanical properties. The temperatures used were −20, +5, and +20 °C, which

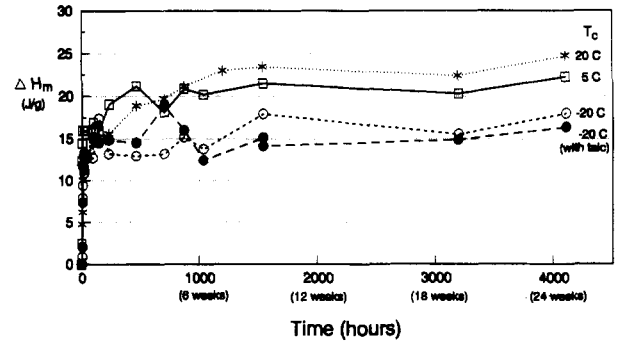

Figure 5. Heat of fusion, ΔH_m, as a function of the 24-week crystallization time for PHO crystallized from the melt at the indicated temperatures including one film containing a possible nucleating agent (0.5% talc).

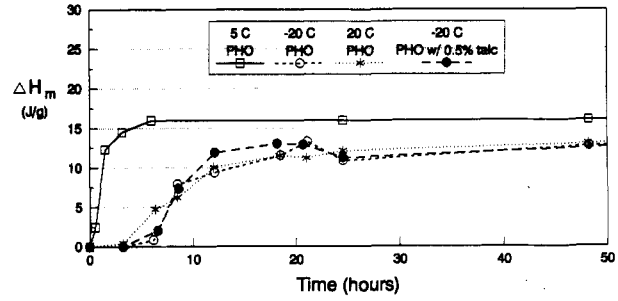

Figure 6. Heat of fusion, ΔH_m, as a function of the first 50 h of crystallization time for PHO crystallized from the melt at the indicated temperatures including one film containing a possible nucleating agent (0.5% talc).

represent slow, fast, and medium crystallization rates, respectively, as determined by the short-term crystallization study. One of the two films crystallized at −20 °C contained a possible nucleating agent, talc, which was included to compare the effect of the possible nucleating agent on the crystallization rate and the final level of crystallinity reached after a long time.

Figure 5 shows the heat of fusion, ΔH_m, as a function of time over the entire 24 weeks of crystallization for all four films. Different maximum levels of crystallinity were reached in each film during the 24 weeks of crystallization, reaching constant levels after approximately 10 weeks. The maximum heat of fusion obtained in the films was directly proportional to the crystallization temperature; larger heats of fusion occurred in films crystallized at higher temperatures.

Results from the initial 50 h are shown more clearly in Figure 6. From this figure, constant levels in the heats of fusion appeared in all the samples. For the film held at 5 °C, this level in the extent of crystallinity was reached after approximately 6 h but took approximately 20 h for the other films. In all cases, the levels were temporary, with a substantial increase in the extent of crystallinity, a 30–100% increase, observed after the entire 24 weeks as shown in Figure 5.

Both films crystallized at −20 °C showed nearly the same final level of crystallinity, with only a slightly lower level of crystallinity observed in the film containing talc. In addition, no significant difference was noted in the time required to develop crystallinity for these two samples (Figures 5 and 6). These observations indicate the talc did not behave as an effective nucleating agent on PHO crystallized from the melt at −20 °C. Perhaps the talc would have affected the crystallization rate more, if the film had been crystallized at a higher temperature where nucleation is limited. In addition, the polymer solution containing the talc had been filtered prior to casting in an

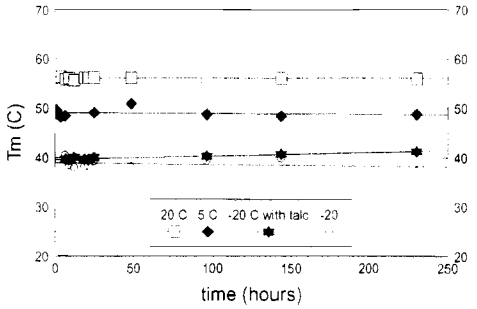

Figure 7. Changes in the peak melting temperature as a function of time.

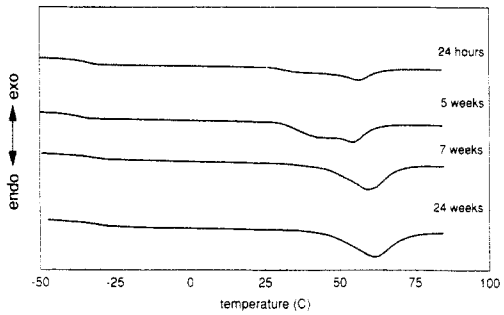

Figure 8. DSC thermograms of PHO crystallized at 20 °C from the melt at various times. These thermograms elucidate changes found for all films over time.

attempt to limit the talc particle size which may have significantly decreased the amount of talc incorporated into the film.

Annealing effects are expected over the 24 weeks because the films were maintained at temperatures above the T_g and below the T_m. Annealing effects observable from DSC experiments are manifested as changes in the shape of the melting endotherm, in the location of the peak melting temperature, and in the area under the endotherm peak.

Monitoring the change in the peak melting temperature over time gave an indication of when annealing effects became significant. From Figure 7, no increase in the melting temperature was observed at PHO crystallized at any crystallization temperature during the first 250 h. Annealing effects were, therefore, not considered significant during the 10-min DSC scans or during the 24-h crystallization study.

The thermograms in Figure 8 illustrate the changes that occurred in the shape of the melting endotherm peaks which were typically observed for all films due to combined crystallization and annealing effects. In general, a broad melting endotherm with an obvious shoulder was at first observed. As crystallization continued, this shoulder became more pronounced and it eventually coalesced into the main peak. The endotherm shown after 24 weeks illustrates the final state of the films prior to mechanical testing.

As expected, the time required for these changes to occur depended on the crystallization temperature, with changes occurring faster at higher temperatures. Table I lists the times taken to maximize the extent and stabilize the melting endotherm shape at the different temperatures. An expected result was that talc significantly shortened the time required to achieve a stable shape in the melting endotherm at −20 °C.

The T_g also increased slightly in all films, by an average of 3–5 °C, with the increase observable only after approximately 250 h. Crystallinity is known to increase the T_g of semicrystalline polymers due to the physical cross-

Table I
Times Associated with Certain Crystallization Parameters

crystallzn temp (°C)	weeks to max extent of crystallzn	weeks to stable melting endotherm peak shape
20	7	7
5	3	16
−20	8	19
−20 with talc	8	9

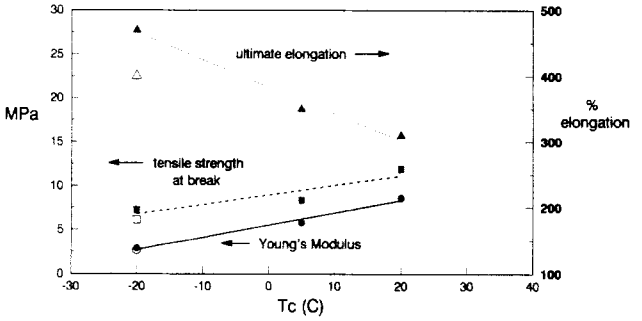

Figure 9. Young's modulus, tensile strength at break, and ultimate elongation as a function of crystallization temperature. Closed symbols represent PHO, and open symbols represent PHO containing talc. Results are average values from ring samples tested at a 1-min^{-1} strain rate.

linking effect these crystalline regions impart on the material.[21]

Mechanical Properties. The results of the effect of crystallization temperature on mechanical properties are shown in Figure 9 where Young's modulus, tensile strength at break, and ultimate elongation are plotted as a function of crystallization temperature. The range of values obtained was large, with Young's modulus showing a 200% increase, tensile strength at break a 60% increase, and ultimate elongation at 50% decrease over the crystallization temperature range evaluated.

The trends in the modulus and ultimate elongation can be explained in terms of the differences in the maximum extent of crystallinity. Higher moduli are expected as the amount of crystallinity increases due to the physical crosslinking and filler effect crystalline regions have on the material.[21] The lower ultimate elongation may be a result of the lower extensibility of crystalline regions, and thus the whole material will become less extensible as the extent of crystallinity increases.

The inclusion of talc significantly decreased the ultimate elongation. However, this effect is believed to be due to a possible flaw in some samples. The material was very soft and tended to extrude out of a small gap in the circular steel rule die. Sample rings containing obvious flaws were not tested. However, slight imperfections in the ring sample could result in premature failure of the material and could be responsible for the observed decrease in both the ultimate elongation and tensile strength at break.

The highest value of Young' modulus observed, approximately 9 MPa obtained with the film crystallized at near room temperature, is almost 100% lower than what was reported in an earlier study (17 MPa).[13] Different strain rates used in testing greatly affected the resulting measured modulus as seen in Figure 10, which shows the sensitivity of the modulus to strain rate. No strain rate was specified in the earlier study, so direct comparison of the earlier value of the modulus with the values determined in this study is inappropriate.

Tensile Set. The tensile set evaluation results are shown in Figure 11. The tensile set was substantial for all films, but a slightly lower tensile set occurred in the

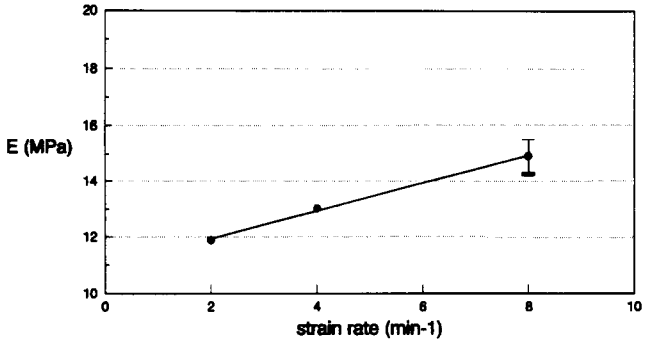

Figure 10. Young's modulus as a function of strain rate for PHO. Results are from strip type samples crystallized at 20 °C from the melt for 24–28 weeks. The error bar represents ±1 standard deviation.

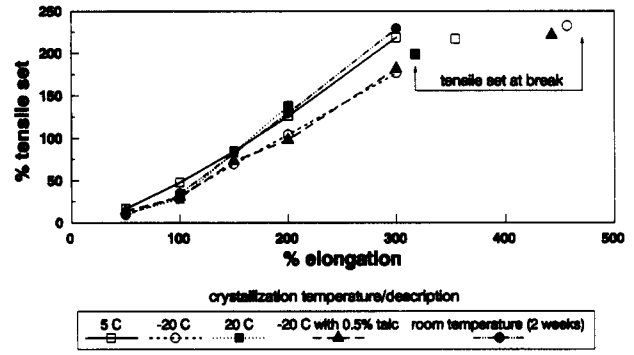

Figure 11. Tensile set evaluation results for PHO crystallized from the melt for 28 weeks at the various temperatures indicated. As a comparison, the tensile set at break values for the films and the tensile set results for PHO crystallized from the melt at room temperature for 2 weeks are also included in the figure.

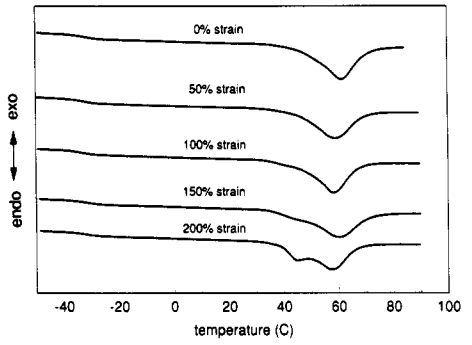

Figure 12. DSC thermograms obtained from PHO films stretched to different elongations. Prior to stretching, the samples were crystallized at 20 °C from the melt for 28 weeks.

material crystallized at −20 °C. As a comparison, the tensile set for PHO crystallized at room temperature for only 2 weeks is included. No difference was noted in the tensile set between PHO crystallized for 2 weeks or extended times. Tensile sets at break are also included in Figure 12.

To investigate the possible reasons for the high tensile set in PHO, thermal analysis was conducted on the strips used in the tensile set measurements from the film which had been crystallized at 20 °C. Samples for the DSC measurements were taken from the stretched region of the strips. Table II lists the DSC results obtained for the samples tested. The heat of fusion initially decreased 10% after 50% elongation, but, upon further elongation, it increased to the initial value prior to elongation. The melting temperature also exhibited a decrease after 50% elongation, with no further decrease observed on samples elongated to higher extents. No change in the glass transition temperature was observed.

Table II
Thermal Analysis Results for PHO Film Crystallized from the Melt at 20 °C and Stretched to Various Elongations[a]

% elongation	ΔH_m (J/g)	T_m (°C) (peak)	T_g (°C) (inflection point)
0	27	62	−32
50	24	59	−32
100	25	58	−33
150	27	59	−32
200	27	58/45	−32

[a] From DSC thermograms at a heating rate of 20 °C/min.

Some unusual changes were observed in the shape in the melting endotherm as seen in Figure 12. A shoulder can be seen forming at the 100% and 150% elongations, but at 200% elongation a new distinct melting peak emerged at a lower melting point, 45 °C. This new peak may indicate that a different crystal structure was formed with stretching. Investigations are continuing to explain the changes in the endotherm peak shape as a function of elongation.

Conclusions

PHO crystallization, based on the heat of fusion as the indicator of the extent of crystallinity, occurred fastest at 0–5 °C. The equilibrium melting point of PHO was determined to be approximately 68 °C. Long-term crystallization is believed to be a combination of crystallization and annealing because the T_g of PHO is below room temperature. PHO crystallized very slowly, requiring approximately 7 weeks at 20 °C and 16 weeks at 5 °C to attain stable levels of crystallinity with an unchanging melting endotherm peak shape.

The thermal history greatly affected the mechanical properties of the material with Young's modulus varying from 2.5 to 9 MPa, tensile strength at break from 6 to 10 MPa, and ultimate elongation from 450% to 300% depending on the crystallization temperature. The tensile set was extensive for PHO crystallized at all three of the temperatures evaluated, approximately 35% after 100% elongation. Elongation of PHO films crystallized for extended times showed unusual changes in the melting endotherm peak shape, and a new distinct, lower melting point peak emerged at 45 °C after 200% elongation. Further studies are being conducted to explain this unusual finding.

Acknowledgment. We thank the Office of Naval Research (Grant No. N00014-86K-0369) and the Procter and Gamble Co., Cincinnati, OH, for their financial support.

References and Notes

(1) Brandl, H.; Gross, R. A.; Lenz, R. W.; Fuller, R. C. *Appl. Environ. Microbiol.* **1988**, *54* (8), 1977.
(2) Gross, R. A.; DeMello, C.; Lenz, R. W.; Brandl, H.; Fuller, R. C. *Macromolecules* **1989**, *22*, 1106.
(3) De Smet, M. J.; Eggink, G.; Witholt, B.; Kingma, J.; Wynberg, H. *J. Bacteriol.* **1988**, *154* (2), 870.
(4) Lageveen, R. G. Dissertation Thesis, University of Groningen, Groningen, The Netherlands, 1986.
(5) Lageveen, R. G.; Huisman, G. W.; Preusting, H.; Ketelaar, P.; Eggink, G.; Witholt, B. *Appl. Environ. Microbiol.* **1988**, *54* (12), 2924.
(6) Huisman, G. W.; DeLeeuw, O.; Eggink, G.; Witholt, B. *Appl. Environ. Microbiol.* **1989**, *55* (8), 1949.
(7) Preusting, H.; Nijenhuis, A.; Witholt, B. *Macromolecules* **1990**, *23*, 4220.
(8) Knee, E. J., Jr.; Wolf, M.; Lenz, R. W.; Fuller, R. C. *Novel Biodegradable Microbial Polymers*; Dawes, E. A., Ed.; Kluwer Academic Publishers: Dordrecht, The Netherlands, 1990; pp 439 and 440.

(9) Holmes, P. A. *Phys. Technol.* **1985**, *16*, 32.
(10) Doi, Y. *Microbial Polyesters*; VCH Publishers, Inc.: New York, 1990; pp 135–150.
(11) Brandl, H.; Gross, R. A.; Lenz, R. W.; Fuller, R. C. *Adv. Biochem. Eng./Biotechnol.* **1990**, *41*, 77.
(12) Ballistreri, A.; Montaudo, G.; Impallomeni, G.; Lenz, R. W.; Kim, Y. B.; Fuller, R. C. *Macromolecules* **1990**, *23*, 5059.
(13) Marchessault, R. H.; Monasterios, C. J.; Morin, F. G.; Sundararajan, P. R. *Int. J. Biol. Macromol.* **1990**, *12* (April), 158.
(14) Bassett, D. C. *Principles of Polymer Morphology*; Cambridge University Press: New York, 1981; pp 124 and 125.
(15) Young, R. J. *Introduction to Polymers*; Chapman and Hall, Ltd.: New York, 1981; pp 193–195.
(16) *Encyclopedia of Polymer Science and Engineering*; John Wiley & Sons: New York, 1985; Vol. 2, p 43.
(17) Gagnon, K. D.; Bain, D. B.; Lenz, R. W.; Fuller, R. C. *Novel Biodegradable Microbial Polymers*; Dawes, E. A., Ed.; Kluwer Academic Publishers: Dordrecht, The Netherlands, 1990; pp 449 and 450.
(18) Gachter, R., Miller, H., Eds. *Plastics Additives Handbook: stabilizers, processing aids, plasticizers, fillers, reinforcements, colorants for thermoplastics*; Hanser Publishers: New York, 1985; pp 671–677.
(19) ASTM D412-87 Standard Test Method for Rubber Properties in Tension.
(20) Barham, P. J.; Keller, A.; Otun, E. L.; Holmes, P. A. *J. Mater. Sci.* **1984**, *19*, 2781.
(21) Nielsen, L. E. *Mechnical Properties of Polymers and Composites*; Marcel Dekker, Inc.: New York, 1974; Vol. 1, p 54.